

Research



Cite this article: Milagre I, Pereira C, Oliveira RA, Jansen LET. 2020 Reprogramming of human cells to pluripotency induces CENP-A chromatin depletion. *Open Biol.* **10**: 200227. <http://dx.doi.org/10.1098/rsob.200227>

Received: 25 July 2020

Accepted: 22 September 2020

Subject Area:

cellular biology/molecular biology/genetics/
developmental biology

Keywords:

centromere, chromatin, CENP-A, iPSC,
human stem cells, kinetochore

Authors for correspondence:

Inês Milagre

e-mail: imilagre@igc.gulbenkian.pt

Lars E. T. Jansen

e-mail: lars.jansen@bioch.ox.ac.uk

Electronic supplementary material is available online at <https://doi.org/10.6084/m9.figshare.c.5172236>.

Reprogramming of human cells to pluripotency induces CENP-A chromatin depletion

Inês Milagre¹, Carolina Pereira¹, Raquel A. Oliveira¹ and Lars E. T. Jansen^{1,2}

¹Instituto Gulbenkian de Ciência, Rua da Quinta Grande, 6, 2780-156 Oeiras, Portugal

²Department of Biochemistry, University of Oxford, OX1, 3QU, UK

IM, 0000-0003-4753-5523; LETJ, 0000-0002-2158-0345

Pluripotent stem cells (PSCs) are central to development as they are the precursors of all cell types in the embryo. Therefore, maintaining a stable karyotype is essential, both for their physiological role as well as for their use in regenerative medicine. Karyotype abnormalities in PSCs in culture are common but the underlying causes remain unknown. To gain insight, we explore the composition of the centromere and kinetochore in human embryonic and induced PSCs. Centromere function depends on CENP-A nucleosome-defined chromatin. We show that while PSCs maintain abundant pools of CENP-A, CENP-C and CENP-T, these essential centromere components are strongly reduced at stem cell centromeres. Outer kinetochore recruitment is also impaired to a lesser extent, indicating an overall weaker kinetochore while the inner centromere protein Aurora B remains unaffected. We further show that, similar to differentiated human cells, CENP-A chromatin assembly in PSCs requires transition into G1 phase. Finally, reprogramming experiments indicate that reduction of centromeric CENP-A levels is an early event during dedifferentiation, coinciding with global chromatin remodelling. Our characterization of centromeres in human stem cells suggests a possible link between impaired centromere function and stem cell aneuploidies.

1. Introduction

Embryonic stem cells (ESCs) are derived from the inner cell mass and can give rise to all cell types in the embryo [1]. The maintenance of genome structure and ploidy is key to their ability to generate viable daughter cells and maintain their differentiation capacity. Despite their extensive proliferative potential, the mechanics of cell division in these cells are still underexplored. One key component for faithful mitosis is the centromere, a specialized chromosomal locus that acts as a chromatin-based platform for the assembly of the kinetochore, composed of microtubule-associated proteins that drive chromosome segregation [2]. How centromere structure is maintained and how it is regulated in stem cells is still unknown.

Pluripotent stem cells (PSCs) can be of embryonic origin; however, they can also be generated in culture using ectopic expression of only four transcription factors [3] leading to the formation of induced PSCs (iPSCs). These share various characteristics with ESCs, such as a truncated cell cycle [4], comparable cell morphology, self-renewal capacities, the expression of pluripotency-associated markers and the ability to differentiate into derivatives of all three primary germ layers [3]. The generation of iPSCs offers key tissue engineering opportunities and clinical applications. Additionally, they also represent a helpful tool in culture to understand how the stem cell state impacts on basic cell biology such as the mechanics of cell division and the fidelity of chromosome segregation.

Induction of pluripotency in differentiated cells requires the repression of somatic genes and activation of self-renewal and pluripotency-associated genes. We and others have shown that reprogramming requires striking remodelling of chromatin modifications, such as global and targeted DNA demethylation at key regulatory regions [5,6], including pluripotency-related enhancers, super-enhancers [6] and histone marks [7]. Specific histone marks, such as H3K4me2 and H3K9me3, are considered barriers to reprogramming as failure to remove or re-distribute these marks results in the inability of cells to reach pluripotency [7]. The profound remodelling of chromatin structure is what allows cells to transition from a somatic cell identity to a stable pluripotent cell identity, while maintaining the same genomic information. It is not clear how this genome-wide remodelling of the chromatin impacts on the structure and stability of the epigenetically defined centromere.

Both human ESCs and iPSCs appear to have an elevated level of genomic instability, at least in culture. Two reports have analysed hundreds of ESC and iPSC lines used in different laboratories worldwide and assessed that at around 10% to as much as 34% of all cell lines have abnormal karyotypes [8,9]. ESCs have a unique abbreviated cell cycle with a shortened G1 phase [10], and the rapid proliferation of these cells has been proposed both as a possible cause, but also as a consequence of these genomic abnormalities [11]. Further, it has been shown that karyotypically abnormal PSCs present defects in the capacity to differentiate into all cell types of the organism and display higher neoplastic capacity, thus hindering their potential application [12]. However, why these cells are prone to karyotypic defects is unclear.

Here we explore the structure of the centromere in both embryo-derived stem cells as well as iPSCs with the aim to understand the basis of mitotic fidelity and possible causes of aneuploidy. Central to the structure, function and maintenance of the centromere is an unusual chromatin domain defined by nucleosomes containing the histone H3 variant CENP-A [13,14]. Centromere specification is largely uncoupled from DNA *cis* elements [15,16] and maintenance depends primarily on a self-propagating CENP-A feedback mechanism [17,18]. We have previously shown in somatic cells that CENP-A is stably associated with chromatin throughout the cell cycle, consistent with a role in epigenetically maintaining centromere position [19,20]. CENP-A chromatin in turn recruits the constitutive centromere-associated network (CCAN) [21,22]. The key components of this network are CENP-C and CENP-T that make direct contacts to the microtubule-binding kinetochore in mitosis [23,24]. CENP-A chromatin propagation is cell cycle regulated and restricted to G1 phase, through inactivation of the cyclin-dependent kinases (Cdk1 and Cdk2) [25,26]. Nascent CENP-A is guided to the centromere by the HJURP chaperone in a manner dependent on the Mis18 complex [27–29], both of which are under strict cell cycle control [26,30].

Although the mechanisms of centromere assembly and the cell cycle control thereof are well established in somatic cells, virtually nothing is known about centromere regulation in PSCs. Here, we define the composition and size of the human centromere in both ESCs as well as iPSCs and find that stem cells maintain a reduced centromeric chromatin size, impacting the key centromere proteins CENP-A, CENP-C and CENP-T, despite ample pools of cellular protein. This reduction in centromere size is recapitulated by induction of the stem cell state and coincides with early reprogramming.

2. Results

2.1. Pluripotent stem cells have a weaker centromere than differentiated cells

To characterize the mitotic performance of ESCs, we cultured the established ESC line H9 (hESCs, henceforth) and determined the fidelity of chromosome segregation. To this end, we fixed and scored mitotic cells for chromosome segregation errors. We compared segregation rates to human retinal pigment epithelium-1 cells (RPE, henceforth) as a representative immortalized somatic epithelial cell line. In agreement with previous reports [8,9], we find that cultured human ESCs have a twofold elevation in total chromosome missegregation events (figure 1*a*).

To characterize centromere size and function in ESCs we compared centromere protein levels by immunofluorescence in hESCs cells and RPE cells in the latter of which we have previously characterized centromeres in detail [31]. Furthermore, we reprogrammed human primary fibroblasts derived from adult skin into iPSCs by Sendai virus-mediated transduction of the Yamanaka reprogramming factors (Oct4, Sox2, Klf4 and c-Myc [3]). We reprogrammed fibroblasts from two different human donors to iPSCs, which express Sox2 and Nanog, to levels comparable to hESCs (electronic supplementary material, figure S1*A*). CENP-A containing nucleosomes form the chromatin platform upon which the centromere complex and kinetochore are built. Despite the essential nature of ESCs to life and development, we find centromeric chromatin to be greatly reduced in CENP-A nucleosomes numbers, at approximately 40% of the levels observed in RPE cells (figure 1*b,c*). Next, we determined whether reduced centromeric chromatin size is unique to hESCs or whether this is a general phenomenon across stem cells. In agreement with the data derived from embryonic stem cells, iPSCs also show a dramatic decline of CENP-A levels at the centromere, to as little as 25% of RPE levels and 29 to 42% of the levels observed in the donor fibroblasts (donor no. 2 and donor no. 1, respectively) from which the iPSCs were reprogrammed (figure 1*b,c*, electronic supplementary material, figure S1*B*). This latter result demonstrates that reduced centromeric CENP-A is directly linked to the epigenetically determined stem cell state as the iPSCs are genetically identical to their cognate donor fibroblasts. To ascertain that the apparent reduction in CENP-A levels is not an antibody accessibility artefact, we complemented these results with cell fractionation experiments. In this orthogonal assay, we observed that hESC have reduced levels of CENP-A in the chromatin bound fraction with a comparative increase in the soluble fraction, when compared to RPE cells (figure 2*a,b*), consistent with the immunofluorescence data.

We have previously determined that human RPE cells have 400 molecules of CENP-A per centromere on average, equating to 200 nucleosomes in interphase [31]. By ratio-metric comparison we estimate CENP-A nucleosome levels at hESCs and the two iPSC lines to be at 80, 70 and 50 nucleosomes per centromere, respectively.

We then determined the impact of the stem cell state on the larger centromere complex. Two key components of the CCAN [2] that make direct contacts with the kinetochore in mitosis are CENP-C and CENP-T [23,24]. Similar to

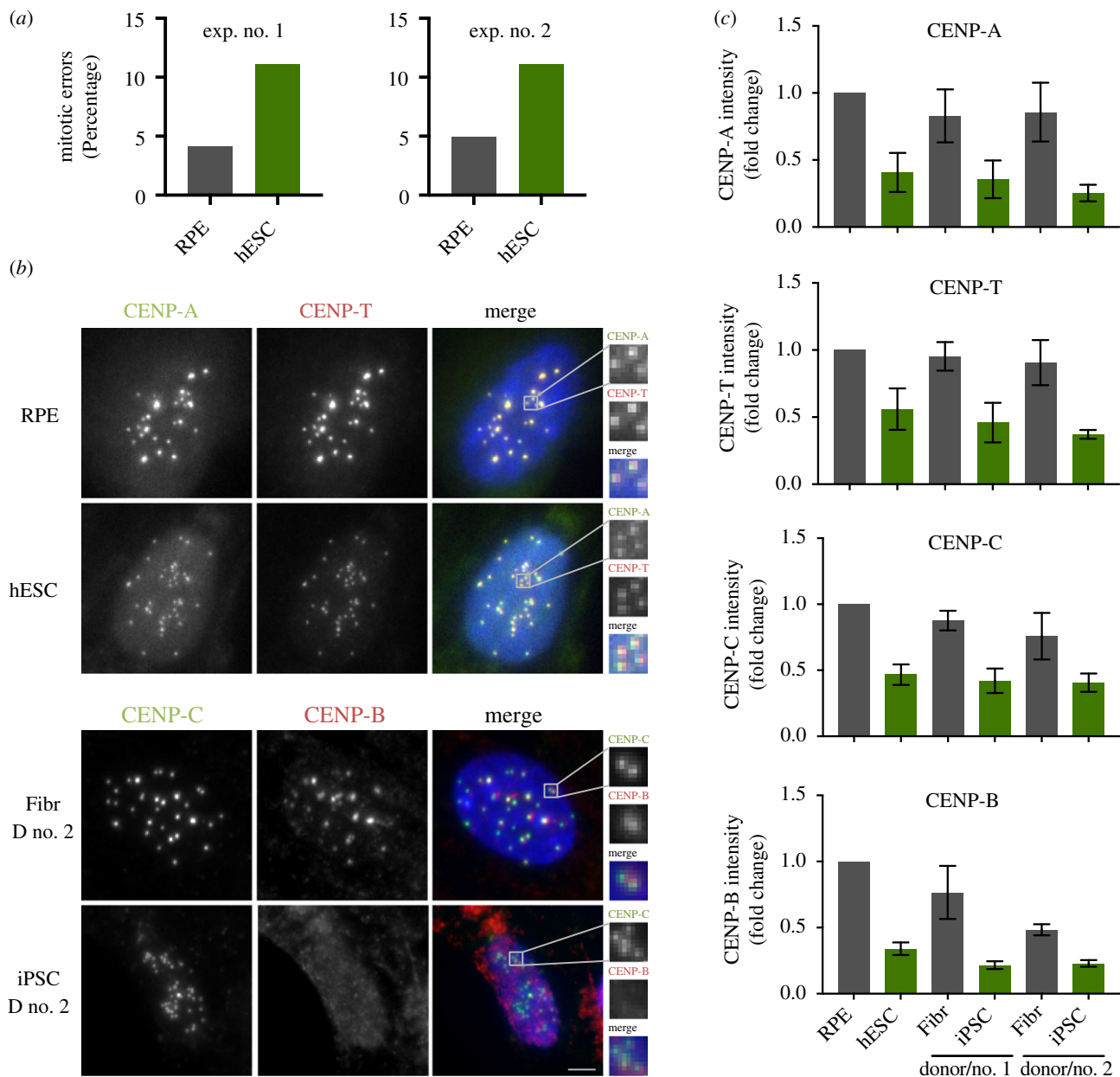


Figure 1. Pluripotent stem cells have a weaker centromere than differentiated cells. (a) Quantification of mitotic errors in RPE and hESC, from two independent experiments. Cells were fixed and the frequency of mitotic errors in unperturbed cells was evaluated. (b) Differentiated (retinal pigment epithelium—RPE and fibroblasts from two independent donors—Fibr D no. 1 and Fibr D no. 2) and pluripotent stem cells (human embryonic stem cell line H9—hESC or iPSC lines reprogrammed from fibroblasts from donor no. 1 and donor no. 2—iPSC D no. 1 or iPSC D no. 2) were fixed and stained for CENP-A, CENP-T, CENP-C or CENP-B and counterstained with DAPI (blue). Representative immunofluorescence images from RPE and human embryonic stem cells (hESCs) are shown for CENP-A and CENP-T and representative images from fibroblasts and iPSC from donor no. 2 are shown for CENP-B and CENP-C. (c) Quantification of centromere intensities as shown in (a) for all cell types. Average centromere intensities were determined using automatic centromere recognition and quantification (CRaQ; see methods). The average and standard error of the mean of three replicate experiments are shown. Centromere intensities are normalized to those of RPE cells. Scale bar = 2 μ m.

CENP-A, we find that both CENP-C and CENP-T levels are dramatically reduced at stem cell centromeres, both in embryonic-derived as well as in iPSCs (figure 1*b,c*; electronic supplementary material, figure S1B). Surprisingly, we find that the direct α -satellite binding protein CENP-B is also reduced at stem cell centromeres to 34% of RPE levels. This is unexpected as CENP-B is, at least in principle, driven by direct DNA sequence contacts [32].

While all centromere components analysed show reduced levels at the centromere, we find this not to be the case for the inner centromere component, Aurora B. This essential mitotic kinase [33] is part of the chromosome passenger complex, localized to the inner centromere and important for error correction during mitosis [34]. We find Aurora B to be

maintained at levels similar to somatic cells (electronic supplementary material, figure S1C and D), indicating that the remodelling at the centromere is unique for the kinetochore forming centromere complex.

One possible explanation for reduced centromere occupancy of CENP-A and CENP-C is that stem cells have reduced expression of centromere protein-encoding genes. To determine expression levels directly, we probed extracts of RPE, hESCs, iPSCs and their parent cells for centromere protein levels. Despite reduced centromere occupancy, both embryonic and induced pluripotent stem cells maintain levels of CENP-A expression, even in excess (up to twofold) of those in fibroblasts, even when compared to genetically identical donor cells of iPSCs (figure 2*c,d*). This

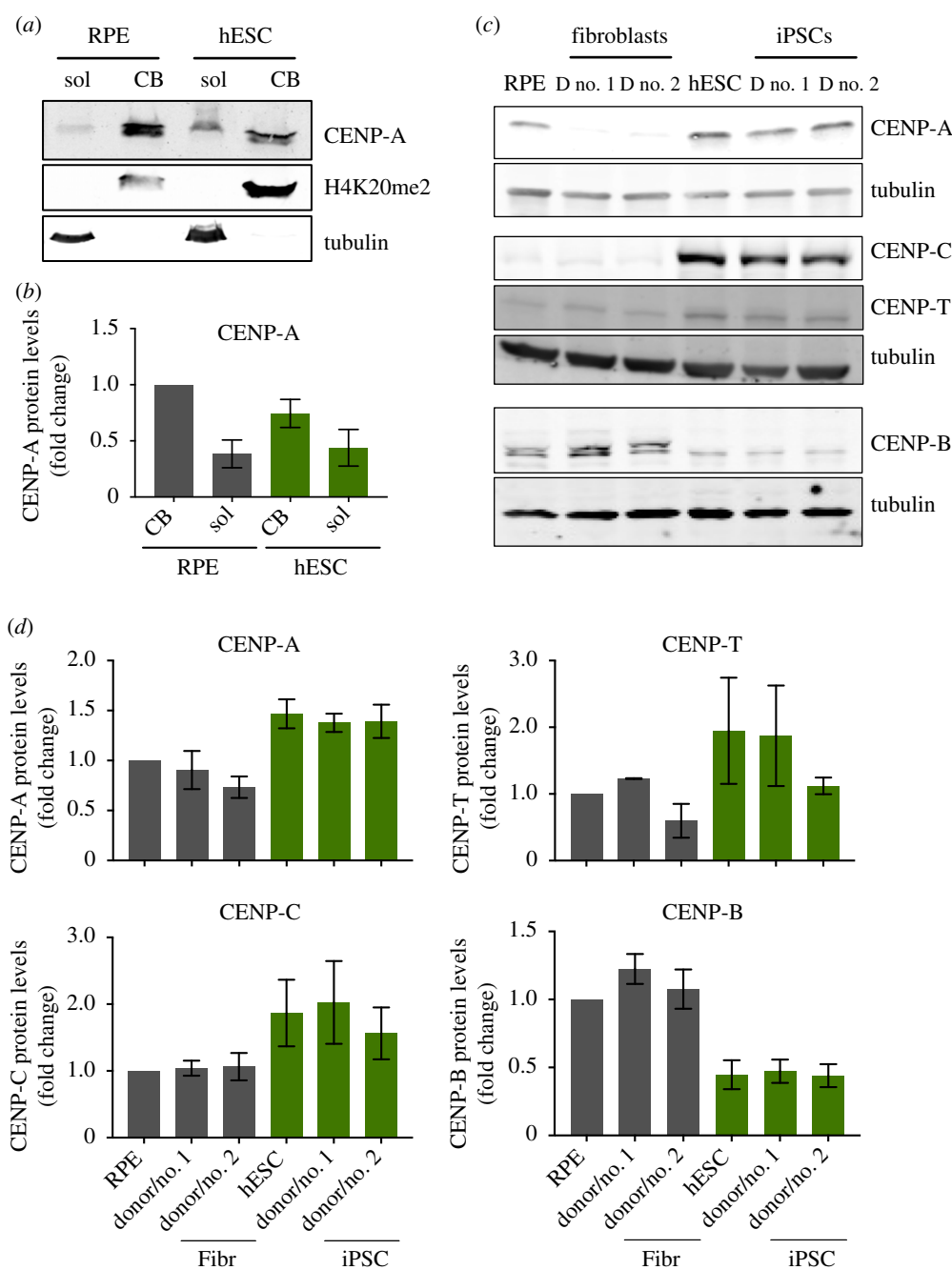


Figure 2. Pluripotent stem cells have elevated expression of CENP-A and CENP-C, and decreased expression of CENP-B. (a) and (b) Cell fractionation experiments to assess total levels of soluble and chromatin bound CENP-A in RPE and hESCs. Immunoblot probed for soluble (sol) and chromatin bound (CB) fractions of CENP-A in RPE and hESCs. Tubulin is used as a marker for the soluble fraction and histone H4K20me2 for the CB fraction (a). Quantification of CENP-A protein levels from six independent experiments (b). (c) Human ESCs, RPE, iPSCs and the fibroblasts they were reprogrammed from, were harvested and processed for SDS-PAGE and immunoblotting. CENP-A, CENP-T, CENP-C and CENP-B levels were assessed with specific antibodies. Tubulin was used as loading control. CENP-A and CENP-E (in figure 4) and CENP-C and CENP-T were detected in the same gel shown using different channels. (d) Quantitation of Western blot bands. The average and standard error of the mean of three replicate experiments are shown. Protein levels were normalized to GAPDH or tubulin.

is consistent with a previous report that evaluated mRNA stores of CENP-A in hESCs [35]. This uncoupling between cellular and centromeric levels in stem cells is also observed for CENP-C as well as CENP-T, albeit with lower confidence, above that of fibroblasts. By contrast, while CENP-B is expressed in stem cells, the overall levels appear to be lower, possibly explaining the reduced centromere levels (figure 2c,d). We note that CENP-B possibly migrates as two species in RPE and fibroblasts but not in stem cells. At present, we do not know the significance of this observation but it may represent a differential modification of CENP-B. In summary, these results indicate that despite large pools of available

CENP-A and CENP-C, these proteins are not efficiently assembled at centromeres.

2.2. CENP-A is loaded in G1 phase of the stem cell cycle

In human differentiated cells, CENP-A has a unique dynamic along the cell cycle, where nucleosomes containing CENP-A are efficiently recycled on sister chromatids during S phase [19,36]. A new assembly of CENP-A occurs exclusively in early G1 phase in a CDK1 and 2 regulated manner [25,26,36]. Human stem cells have a characteristically abbreviated cell cycle where cells enter S phase soon after exiting

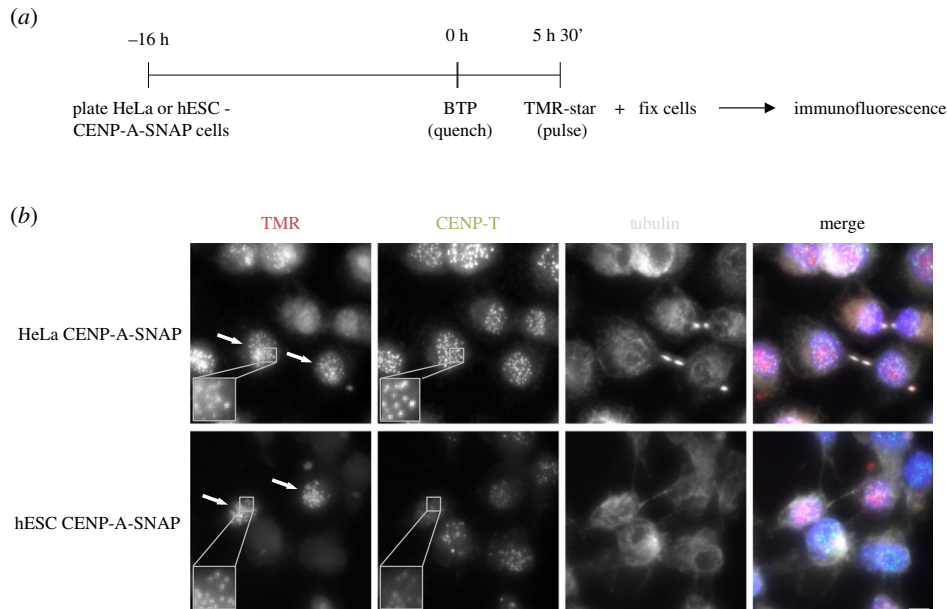


Figure 3. CENP-A assembles in the canonical G1 phase of the pluripotent stem cell cycle. (a) SNAP-tag based quench-chase-pulse labelling: CENP-A-SNAP expressing hESC or HeLa cells were labelled with the non-fluorescent substrate (BTP; quench) followed by a chase period (5 h 30 min) during which new unlabelled protein is synthesized. Nascent protein is subsequently fluorescently labelled with TMR-Star (Pulse). Localization and fate of nascent fluorescently labelled CENP-A-SNAP is determined by high-resolution microscopy. (b) Representative fluorescence images of differentiated (HeLa-CENP-A-SNAP) cells or hESCs (hESC CENP-A-SNAP) as processed according to (a). Tubulin staining was used to identify midbodies, indicative of G1 phase cells. CENP-A-SNAP assembly occurs in a subset of cells and all midbody positive cells are positive for nascent CENP-A assembly. Arrows indicate cells in G1. Scale bar = 5 μm .

from mitosis [10]. As G1 phase is short in these cells, CENP-A assembly dynamics could be altered. We determined the timing of CENP-A assembly using a previously established CENP-A assembly assay based on SNAP enzyme fluorescent quench-chase-pulse labelling [37]. We established an hESC line in which we introduced a SNAP-tagged CENP-A transgene by piggyBac transposition to avoid gene silencing in stem cells [38] see methods. We then subjected cells to a SNAP quench-chase-pulse protocol in which only nascent CENP-A-SNAP is visualized (figure 3a). Cells were co-stained with α -tubulin to mark microtubules and identify G1 cells, based on the characteristic G1-phase-specific midbody staining. This analysis revealed that cells in G1 are positive for CENP-A assembly, similar to control somatic HeLa-CENP-A-SNAP cells (figure 3b and [25,26,36]). We therefore conclude that the G1-phase assembly is preserved in embryonic stem cells.

2.3. Mild reduction of kinetochore size of pluripotent stem cells in mitosis

As we find hESCs and iPSCs to maintain a much smaller centromere complex, we determined the consequences for kinetochore size which is the key protein complex to generate microtubule attachments in mitosis [2]. We stained mitotic cells for CENP-E, a mitotic kinesin, critical for chromosome congression [39]. Further, we determined the levels of HEC1, an essential component of the KNL-1/Mis12 complex/Ndc80 complex (KMN) network of proteins, responsible for microtubule binding [40] (figure 4a). Both proteins accumulate on mitotic kinetochores in stem cells. While CCAN levels are low (figure 1), both outer kinetochore components analysed are only modestly reduced compared to epithelial RPE cells or donor fibroblasts (figure 4b,c). Cells were analysed at similar mitotic stages to avoid any cell cycle effects on kinetochore

levels. Interestingly, similar to the excess cellular pools of CENP-A and CENP-C, we find that the reduced kinetochore is not a consequence of a lack of expression as overall levels of both CENP-E, as well as HEC1, are higher in stem cells and iPSCs compared to RPE or fibroblasts (figure 4d,e).

2.4. CENP-A loss is induced during early reprogramming of fibroblasts to induced pluripotent stem cells

The ability to induce the stem cell state in differentiated cells offers a unique opportunity to determine the dynamics of centromeric chromatin organization and how this is linked to the formation of stem cells. The comparison of CENP-A chromatin in iPSCs and their cognate donor cells suggest that CENP-A loss is an epigenetic event that occurs during reprogramming of otherwise genetically identical cells. To determine when during the reprogramming process CENP-A loss occurs, we transduced fibroblasts with a cocktail of Sendai viruses expressing the four Yamanaka factors to induce pluripotency (figure 5a). Complete iPSC formation typically requires 30 days of culturing followed by clone isolation at 40–60 days (figure 5a). Here, we focused on very early signs of reprogramming based on the expression of the pluripotency marker SSEA-4, which becomes expressed early during dedifferentiation [41]. Fibroblasts do not express this cell surface protein; however, they express CD13 (which is not expressed in PSCs). Taking advantage of this, we used fluorescence-activated cell sorting (FACS) to isolate SSEA-4 negative/CD13 positive (refractory to reprogramming) or SSEA-4 positive/CD13 negative (prone to reprogramme) cells as early as 9 and 11 days post-transduction of reprogramming factors (figure 5a). These cells were stained for CENP-A, CENP-B and CENP-C to determine centromeric levels of the CCAN.

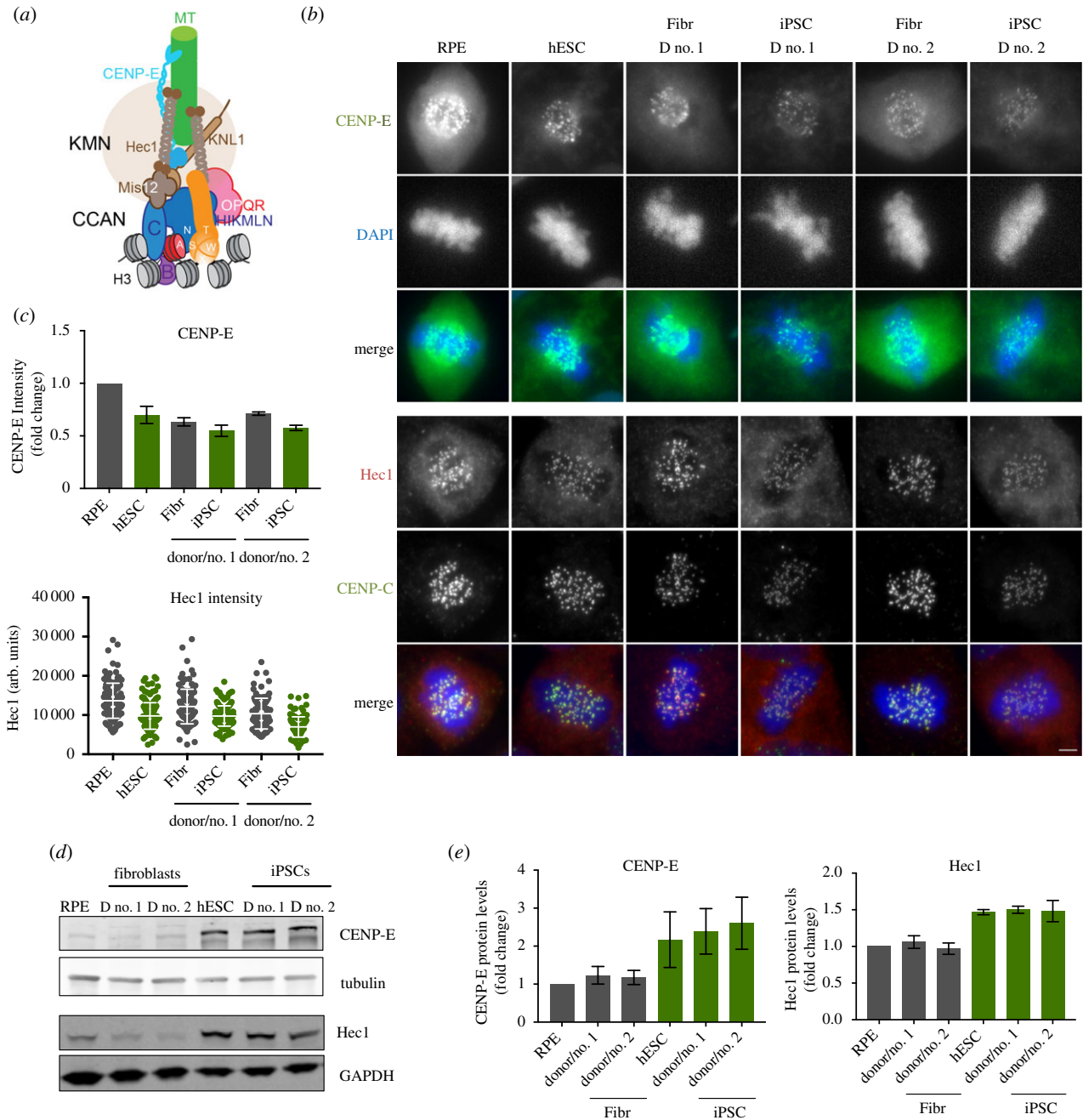


Figure 4. Reduced outer kinetochore size of PSCs in mitosis. (a) Scheme representing the architecture and interactions of different proteins that comprise the human centromere and kinetochore. (b) Representative immunofluorescence images from differentiated (RPE and fibroblasts derived from donor no. 1 and donor no. 2—Fibr D no. 1 and Fibr D no. 2) and pluripotent stem cells (human embryonic stem cell line H9—hESC and iPSCs reprogrammed from Fibr D no. 1 and Fibr D no. 2—iPSC D no. 1 and iPSC D no. 2) for CENP-E and Hec1. (c) Quantitation of centromeric CENP-E and Hec1. Mean levels of fluorescence per nuclei was measured (CENP-E) or average centromere intensities were determined using automatic centromere recognition and quantification (Hec1). The average and standard error of the mean of one (Hec1) or three (CENP-E) independent experiments are shown. (d) Human ESCs, RPE, iPSCs and the fibroblasts they were reprogrammed from, were harvested and processed for SDS-PAGE and immunoblotting. CENP-E and Hec1 levels were assessed with specific antibodies. GAPDH (Hec1) or tubulin (CENP-E) was used as a loading control. CENP-E and CENP-A (in figure 2) were detected in the same gel shown using different channels. (e) Quantitation of WB bands. Average and standard error of the mean of three independent experiments are shown. Protein levels were normalized to GAPDH or tubulin. Scale bar = 2 μ m.

We find that as early as 9 days, the first time point at which we can isolate a significant amount of SSEA-4 positive/CD13 negative cells, CENP-A levels show signs of decline which become more evident at 11 days post-transduction (figure 5*b, c*). CENP-B and to a lesser extent CENP-C levels, also follow this pattern of recruitment to the centromere, with CENP-B levels decreasing as early as day 9 of reprogramming (figure 5*b, c*). These results indicate that the reorganization of centromeres is tightly linked to the stem cell state and correlates with early reprogramming events.

3. Discussion

The centromere is an essential chromosomal locus to drive chromosome segregation. While its structure and function has been studied in considerable detail in somatic, differentiated cells of different organisms, e.g. cancer cells, immortalized cells and primary cells in humans, chicken DT40 lymphocytes and *Drosophila* tissue culture cells [13,42], relatively little is known about centromere structure in stem cell populations. Aspects of centromere biology have been reported in stem

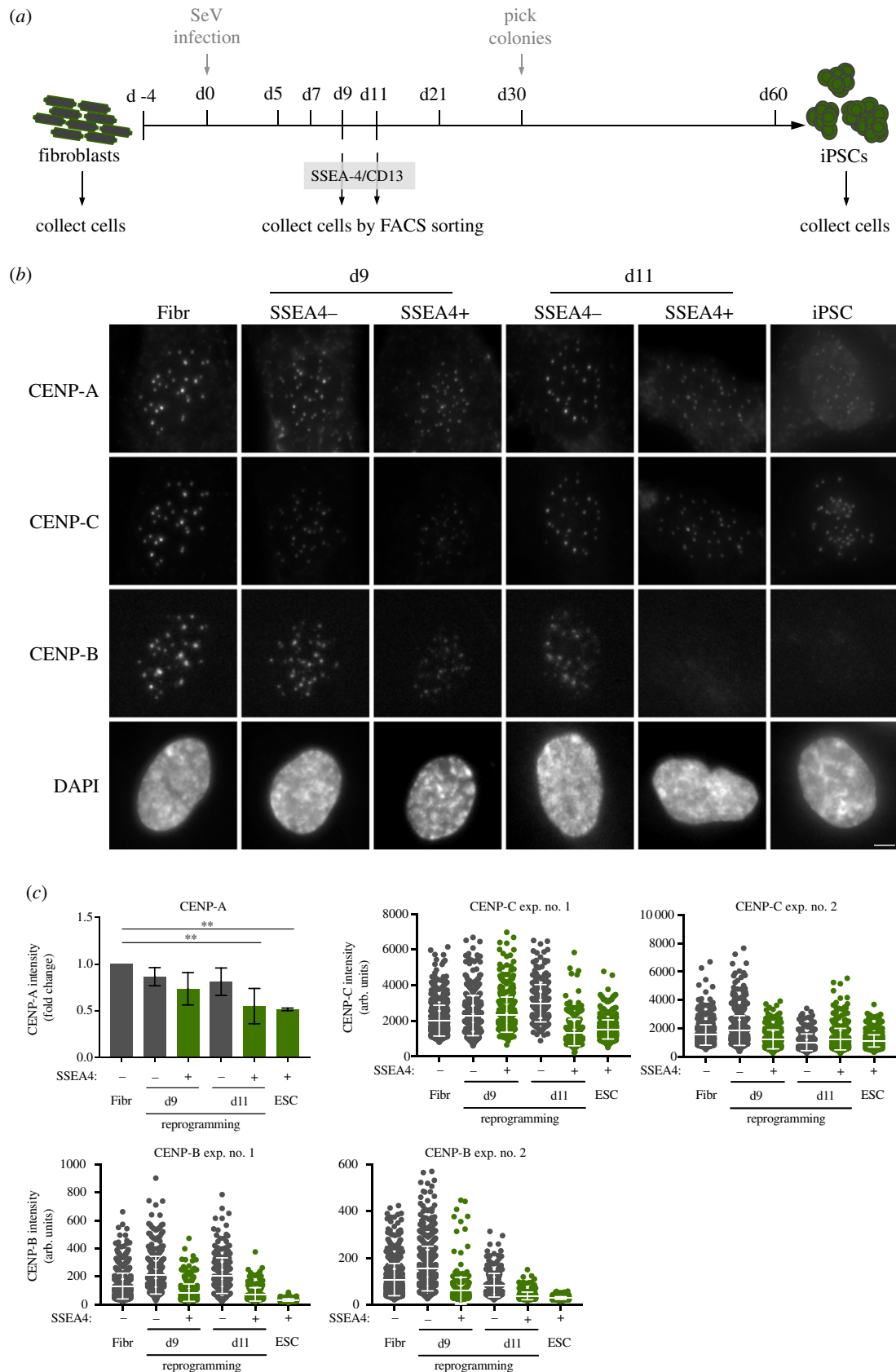


Figure 5. CENP-A loss is induced during early reprogramming of fibroblasts to iPSCs. (a) Outline of the general strategy to reprogramme iPSCs from fibroblasts: human primary fibroblasts are reprogrammed by infection with Sendai virus (SeV) expressing Oct4, Sox2, Klf4 and c-Myc. At days 9 and 11 after infection (d9 and d11, respectively), cells are incubated with antibodies specific for SSEA-4 (early pluripotency marker) and CD13 (fibroblast marker) and collected by FACS sorting. Thirty days after infection, visible colonies appear and can be picked under the microscope. Single colonies are picked, expanded and kept in culture. The cells collected at days 9 and 11, the initial fibroblast population and fully reprogrammed iPSCs (reprogrammed from those fibroblasts), were stained for CENP-A, CENP-B and CENP-C and counterstained with DAPI. (b) Representative immunofluorescence images from cells collected by FACS at d9 and d11 and sorted by pluripotency profile (SSEA4 negative and CD13 positive—refractory to reprogramming—versus SSEA4 positive and CD13 negative cells—prone to reprogram) and control cells. (c) Quantification of centromere intensities as shown in (b). Average centromere intensities were determined using automatic centromere recognition and quantification (CRaQ; see methods) for indicated cell types. For CENP-A, the average and standard error of the mean of three replicate experiments is shown for indicated cell types. For CENP-B and CENP-C, two experiments were performed and analysed. Horizontal lines represent the mean, and whiskers represent standard deviation, for each sample. Scale bar = 2 μ m.

cells of the *Arabidopsis* meristem and *Drosophila* midgut and male germline [43–45], but centromere structure and size has not been thoroughly investigated in those systems.

Using human ESCs and iPSCs as a model, we found that these cells maintain a low level of centromeric chromatin as well as associated centromere proteins, despite abundant cellular pools. Interestingly, the inner centromere component Aurora B is maintained at normal levels and does not seem affected in PSCs. Moreover, we find that the weak centromere seems to only moderately affect the recruitment of kinetochore proteins in mitosis. These findings indicate that CCAN size and kinetochore size regulation can be uncoupled, and that stem cells have the ability to partially, but not fully, compensate for the reduced centromeric chromatin size. Although this does not seem to be a conserved characteristic of the centromere [46], we previously showed this to be the case in RPE cells in which forced reduction or expansion of CENP-A chromatin had little impact on kinetochore size [31]. We now find a physiological example of a partial compensatory mechanism within the kinetochore.

It has previously been shown that, in *Drosophila*, CENP-A assembles in telophase/early G1 in brain stem cells [47]. An increase in CENP-A in G2 in germline stem cells has also been suggested recently [45]. Here, we show that assembly of CENP-A chromatin occurs in G1 phase of the stem cell cycle, as is the case in human differentiated and immortalized cells and in cancer cell lines [25,36]. An open question remains how CENP-A levels are restricted in stem cells. One possibility is that cells that exit mitosis and rapidly transition into S phase have a relatively short G1 phase window during which CENP-A can be assembled before inhibitory Cdk activity rises [25]. It is tempting to speculate that this combined with the lack of CENP-B, could lead to the destabilization of CENP-A and CENP-C [48], resulting in a weaker centromere in PSCs. As cells differentiate, G1 phase becomes elongated potentially allowing more CENP-A to be assembled. However, testing this directly in PSCs by extending G1 has the confounding effect to also leading cells to differentiate as the pluripotency state and the short cell cycle are intrinsically linked [49].

We further find that reduction in centromeric chromatin size is induced early during iPSC reprogramming, coincident with the time of cell cycle shortening. Profound remodelling of chromatin marks is observed during reprogramming and one of the earliest events in reprogramming is the rapid genome-wide re-distribution of H3K4me2 during both mouse and human somatic cell reprogramming [50,51]. Moreover, methylation of H3K4me2 by Wrd5 to a trimethylated state, leading to a global decrease in di-methylation, is required for both self-renewal and efficient reprogramming of somatic cells [52]. H3K4me2 depletion at engineered centromeric chromatin causes defects in HJURP recruitment and CENP-A assembly and consequent kinetochore dysfunction and chromosome missegregation [53]. These and other major chromatin changes that also occur during this early window, including DNA methylation erasure, could play a role in CENP-A chromatin remodelling. Conversely, we would predict that the reduced levels of centromeric CENP-A and associated proteins would be regained upon differentiation although the rate at which this happens remains to be tested.

Finally, cultured stem cells are prone to chromosome missegregation compared to differentiated cells. While this can be a consequence, at least in part, of cell culture conditions, our findings that stem cells maintain a reduced centromere

complex, may impact on chromosome segregation fidelity. However, we find that levels of kinetochore proteins are only modestly reduced and Aurora B in the inner centromere is maintained. Therefore, any mitotic defects are not expected to be dramatic. The key defect relates to very low CENP-B levels, a condition comparable to the Y chromosome or neo-centromere-containing chromosomes, lacking CENP-B [54,55]. While CENP-B is not strictly essential for viability, somatic cells have been reported to missegregate these chromosomes at a low frequency [48]. Full deletion of CENP-B leads to modest loss of CENP-A and CENP-C [48], which is analogous to the situation we reveal in stem cells. We therefore postulate that low CENP-A, -B and -C levels may be sufficient to impact on chromosome segregation efficiency even if kinetochore levels are only modestly affected and the inner centromere is maintained.

4. Material and methods

4.1. Cell culture

All cell lines were grown at 37°C in 5% CO₂ incubators. Normal human dermal fibroblasts (NHDF - GIBCO) were maintained in fibroblast medium (Dulbecco's modified Eagle's medium (DMEM) high glucose, 10% foetal bovine serum (FBS), 1% Pen-Strep, 1% minimum essential medium (MEM) non-essential amino acids and 50 µM 2-mercaptoethanol). H9 ESC (hESC) and hiPSC lines were grown in vitronectin (VTN) coated plates in Essential-8 medium (TeSR-E8, Stem Cell Technologies), and dissociated with gentle cell dissociation reagent (0.5 mM ethylenediamine tetraacetic acid (EDTA) in phosphate buffered saline (PBS)) or Tryple-Express Enzyme (Gibco) when single-cell dissociation was necessary. RPE-1 cells were grown in RPE medium (DMEM/F-12, 10%FBS, 1% Pen-Strep, 2 mM L-glutamine, 1.6% sodium bicarbonate). HeLa-CENP-A SNAP clone no. 72 [36] was grown in HeLa medium (DMEM high glucose, 10% FBS, 1% Pen-Strep, 2 mM L-glutamine).

4.2. Reprogramming of human fibroblasts to induced pluripotent stem cells

Reprogramming was performed as described previously [6]. Briefly, 3.0×10^5 normal human dermal fibroblasts (NHDFs) were transduced with CytoTune®-iPS 2.0 Sendai Reprogramming Kit (Invitrogen), according to manufacturer's instructions, at a multiplicity of infection of 1. Cells were maintained in fibroblast medium (DMEM, 10% FBS, 1% Pen-Strep, 1% MEM non-essential amino acids and 50 µM 2-mercaptoethanol) for 5 days. Transduced cells were then replated onto VTN (Invitrogen)-coated dishes and maintained in Essential 8 medium (E8 - stem cell technologies). Medium was replenished daily. Cells were collected at different time-points during reprogramming by FACS (d9, d11) or manually (NHDFs and fully established iPSCs).

4.3. Immunofluorescence, microscopy and image analysis

Cells were grown on glass coverslips coated with poly-L lysine (Sigma-Aldrich) or VTN (Thermo Fischer Scientific) and fixed with 4% formaldehyde (Thermo Scientific) for 10 min followed

by quenching with 100 mM Tris-HCl. Cells were permeabilized in PBS with 0.3% Triton-X-100. All primary antibody incubations were performed at 37°C for 1 h in a humid chamber. Fluorescent secondary antibodies were from Jackson ImmunoResearch (West Grove, PA) or Rockland Immuno-Chemicals (Limerick, PA) and used at a dilution of 1:250. All secondary antibody incubations were performed at 37°C for 45 min in a humid chamber. Cells were counter-stained with DAPI (4',6-diamidino-2-phenylindole; Sigma-Aldrich) before mounting in Mowiol.

The following primary antibodies and dilutions were used: mouse monoclonal anti-CENPA (no. ab13939, abcam) at 1:500, rabbit polyclonal anti-CENP-B (no. ab25734, Abcam) at 1:500, guinea-pig polyclonal anti-CENP-C (no. PD030, MBL International) at 1:1000, rabbit polyclonal anti-CENP-T at 1:250 (no. ab220280, Abcam), goat anti-Sox2 (no. AF2018, R&D) at 1:200, goat anti-Nanog (no. AF1997, R&D) at 1:100, rabbit anti-CENP-E (kind gift from Don Cleveland) at 1:200, mouse monoclonal anti-Aurora B (no. 611082, BD Transduction Laboratories) at 1:200, mouse monoclonal anti-HEC1 (Thermo Scientific Pierce MA1-23308) at 1:100 and rat monoclonal anti- α -tubulin (SC-53029, Santa Cruz Biotechnology, Dallas, TX) at 1:10 000.

Z-stack slices were captured with wide-field microscopes, either a Leica High Content Screening microscope, based on Leica DMI6000 equipped with a Hamamatsu Flash Orca 4.0 sCMOS camera, using a 63 \times oil objective (HC PLAN APO, NA 1.4) with 0.2 μ m z sections, or a Deltavision Core system (Applied Precision) inverted microscope (Olympus, IX-71) coupled to a Cascade2 EMCCD camera (Photometrics), using a 60 \times oil objective (Plan Apo N, NA 1.42) with 0.2 μ m z sections.

Immunofluorescent signals were quantified using the Centromere Recognition and Quantification method [37] using CENP-A, CENP-T or CENP-C as centromeric reference. Alternatively, CENP-E levels were measured only in mitotic cells using an IMAGEJ based macro, which measures the median intensity of the whole nucleus.

4.4. Immunoblot analysis

Whole-cell extracts were resolved by SDS-PAGE and blotted onto Nitrocellulose membranes. Membranes were blocked in TBS-Tween (10% powdered milk) or Odyssey blocking buffer (Li-cor Biosciences) and incubated overnight at 4°C with the indicated antibodies. Secondary antibodies were used at 1:10 000 prior to detection on Odyssey near-infrared scanner (Li-cor Biosciences).

The following primary antibodies were used for immunoblot: rabbit polyclonal anti-CENP-A (no. 2186, Cell Signaling Technology) at 1:500, rabbit polyclonal anti-CENP-B (no. ab25734, Abcam) at 1:200, rabbit polyclonal anti-CENP-T (no. ab220280, Abcam) at 1:250, guinea pig polyclonal anti-CENP-C (no. PD030, MBL International) at 1:250, rabbit polyclonal anti-H4K20me (no. ab9052, Abcam) at 1:4000, rabbit anti-CENP-E (kind gift from Don Cleveland) 1:250, mouse monoclonal anti-Hec1 (no. MA1-23308, Thermo Fischer Scientific) at 1:250, mouse monoclonal anti- α tubulin (T9026, Sigma-Aldrich) at 1:5000 and rabbit monoclonal anti-GAPDH (no. 2118S, Cell Signaling) at 1:2000. Secondary antibodies used: IRDye800CW anti-rabbit (Li-cor Biosciences), IRDyLight800CW anti-rabbit (Li-cor Biosciences), IRDyLight800CW anti-guinea (Li-cor Biosciences), IRDyLight800CW

anti-mouse (Li-cor Biosciences) and IRDyLight680LT anti-mouse (Li-cor Biosciences).

4.5. Cell fractionation

Cell fractionation was performed for RPE and hESC lines after cell lysis in ice-cold buffer (50 mM Tris-HCl (pH 7.5), 150 mM NaCl, 0.5 mM EDTA, 1% Triton-X 100 and a protease inhibitor cocktail (ROCHE)). Soluble proteins were separated from the insoluble fraction by centrifugation at 21 100g at 4°C and resuspended in an equal volume of lysis buffer. Pellet fraction was incubated with 1.25 U μ l⁻¹ of benzoylase nuclease (Merck, Millipore, Burlington, MA) on ice for 10 min prior to denaturation in 4X loading buffer (Li-Cor).

4.6. DNA constructs

To obtain the hESC CENP-A-SNAP cell line, we re-cloned CENP-A-SNAP, from pBABE-CENP-A SNAP plasmid [36], to avoid retroviral silencing, onto a piggyBac plasmid (pB-CAG-Dest-pA-pgk-bsd - kind gift from José Silva).

4.7. Stable cell lines

hESC H9 cell line was transfected with 2 μ g of pB-CAG-Dest-pA-pgk-bsd-CENP-A-SNAP plus 2 μ g of pBASE plasmid (harbouring the piggyBac transposase, kind gift from José Silva) using FuGeneHD (Roche), in a ratio of DNA : FuGene of 1 : 3. Cells were then subjected to 5 days blasticidin selection and single clones were picked and characterized for CENP-A-SNAP protein levels by immunoblot.

4.8. Quench-chase-pulse labelling

Cell lines expressing CENP-A-SNAP were quench-pulse labelled as previously described [37]. Briefly, cells were quenched with a non-fluorescent bromothenylpteridine (BTP; New England Biolabs) at 2 μ M final concentration and kept in culture for 5 h and 30 min. Cells were then pulse labelled with tetra-methyl-rhodamine-conjugated SNAP substrate (TMR-Star; New England Biolabs) at 4 μ M final concentration, labelling all newly synthesized CENP-A molecules at the centromere, and fixed for immunofluorescence.

4.9. Fluorescence-activated cell sorting

For cell sorting, cells undergoing reprogramming were incubated with antibodies against CD13 (PE, BD Pharmigen) and SSEA-4 (Alexa Fluor 647, BD Pharmigen) for 30 min. Cells were washed in a 2% FBS/PBS solution and passed through a 50 μ m cell strainer to obtain a single-cell suspension.

Appropriate negative and positive controls were used to assess optimal FACS conditions. Cell sorting was performed using a FACSAria cell sorter instrument (BD Biosciences) and cells were collected for immunofluorescence. All flow cytometry experiments were performed at the flow cytometry facility of Instituto Gulbenkian de Ciência, Oeiras, Portugal.

Ethics. All experiments were carried out with the approval of the IGC Ethics committee and in compliance with EU and national legislation on ethics in research. The human embryonic stem cell line H9 was purchased from the official distributor (WiCell, USA), with the certification that the cells were ethically obtained. This cell line is already established and has been registered in the European human pluripotent

stem cell registry (<http://hpscreg.eu/cell-line/WAe009-A>). Fibroblasts from human donors were obtained from commercial sources, with the certification that all tissues used for human cell products is ethically obtained with documented, informed donor consent.

Data accessibility. Raw data, uncropped immunoblots are provided as the electronic supplementary material document.

Authors' contributions. I.M. conceived the project, designed and performed experiments, analysed data and wrote the manuscript; C.P. performed immunoblot and cell fractionation experiments, R.A.O and L.E.T.J. interpreted the data, provided helpful discussions for project design and wrote the manuscript. All authors have interpreted the data and provided helpful discussions, read and approved the manuscript.

Competing interests. We declare we have no competing interests.

Funding. This work was funded by Fundação para a Ciência e Tecnologia project: PTDC/BIA-CEL/31502/2017 and was supported by the European Union's Horizon 2020 research and innovation programme under the Marie Skłodowska-Curie grant agreement no.

704763 (fellowship to I.M.), as well as funding from an ERC-consolidator grant ERC-2013-CoG-615638 and a Wellcome Senior Research Fellowship in Basic Biomedical Science to L.E.T.J. and EMBO Installation Grant IG2778 to R.A.O.

Acknowledgements. We thank José Silva (Cambridge Stem Cell Institute) for the pB-CAG-Dest-pA-pgk-bsd and pBASE plasmids, Don W. Cleveland (UCSD) for CENP-E antibodies and João Mata (IGC) for technical support. We would like to thank the members of the Jansen and Oliveira laboratories for helpful discussions and acknowledge the technical support of IGC's Advanced Imaging Facility (AIF-UIC), which is supported by the national Portuguese funding ref no. PPBI-POCI-01-0145-FEDER-022122, co-financed by Lisboa Regional Operational Programme (Lisboa 2020), under the Portugal 2020 Partnership Agreement, through the European Regional Development Fund (FEDER) and Fundação para a Ciência e a Tecnologia (FCT; Portugal). We would like to thank the Flow Cytometry Facility of Instituto Gulbenkian de Ciência for their services and assistance.

References

- Thomson JA, Itskovitz-Eldor J, Shapiro SS, Waknitz MA, Swiergiel JJ, Marshall VS, Jones JM. 1998 Embryonic stem cell lines derived from human blastocysts. *Science* **282**, 1145–1147. (doi:10.1126/science.282.5391.1145)
- Cheeseman IM, Desai A. 2008 Molecular architecture of the kinetochore–microtubule interface. *Nat. Rev. Mol. Cell Biol.* **9**, 33–46. (doi:10.1038/nrm2310)
- Takahashi K, Yamanaka S. 2006 Induction of pluripotent stem cells from mouse embryonic and adult fibroblast cultures by defined factors. *Cell* **126**, 663–676. (doi:10.1016/j.cell.2006.07.024)
- Ghule PN *et al.* 2011 Reprogramming the pluripotent cell cycle: restoration of an abbreviated G1 phase in human induced pluripotent stem (iPS) cells. *J. Cell. Physiol.* **226**, 1149–1156. (doi:10.1002/jcp.22440)
- Lee D-S *et al.* 2014 An epigenomic roadmap to induced pluripotency reveals DNA methylation as a reprogramming modulator. *Nat. Commun.* **5**, 5619. (doi:10.1038/ncomms6619)
- Milagre I *et al.* 2017 Gender differences in global but not targeted demethylation in iPSC reprogramming. *Cell Rep.* **18**, 1079–1089. (doi:10.1016/j.celrep.2017.01.008)
- Nashun B, Hill PWS, Hajkova P. 2015 Reprogramming of cell fate: epigenetic memory and the erasure of memories past. *EMBO J.* **34**, 1296–1308. (doi:10.15252/embj.201490649)
- International Stem Cell Initiative *et al.* 2011 Screening ethnically diverse human embryonic stem cells identifies a chromosome 20 minimal amplicon conferring growth advantage. *Nat. Biotechnol.* **29**, 1132–1144. (doi:10.1038/nbt.2051)
- Taapken SM, Nisler BS, Newton MA, Sampsel-Barron TL, Leonhard KA, McIntire EM, Montgomery KD. 2011 Karyotypic abnormalities in human induced pluripotent stem cells and embryonic stem cells. *Nat. Biotechnol.* **29**, 313–314. (doi:10.1038/nbt.1835)
- Becker KA, Ghule PN, Therrien JA, Lian JB, Stein JL, van Wijnen AJ, Stein GS. 2006 Self-renewal of human embryonic stem cells is supported by a shortened G1 cell cycle phase. *J. Cell. Physiol.* **209**, 883–893. (doi:10.1002/jcp.20776)
- Weissbein U, Benvenisty N, Ben-David U. 2014 Quality control: genome maintenance in pluripotent stem cells. *J. Cell Biol.* **204**, 153–163. (doi:10.1083/jcb.201310135)
- Zhang M, Cheng L, Jia Y, Liu G, Li C, Song S, Bradley A, Huang Y. 2016 Aneuploid embryonic stem cells exhibit impaired differentiation and increased neoplastic potential. *EMBO J.* **35**, 2285–2300. (doi:10.15252/embj.201593103)
- McKinley KL, Cheeseman IM. 2016 The molecular basis for centromere identity and function. *Nat. Rev. Mol. Cell Biol.* **17**, 16–29. (doi:10.1038/nrm.2015.5)
- Mitra S, Srinivasan B, Jansen LET. 2020 Stable inheritance of CENP-A chromatin: inner strength versus dynamic control. *J. Cell Biol.* **219**, e202005099. (doi:10.1083/jcb.202005099)
- Marshall OJ, Chueh AC, Wong LH, Choo KHA. 2008 Neocentromeres: new insights into centromere structure, disease development, and karyotype evolution. *Am. J. Hum. Genet.* **82**, 261–282. (doi:10.1016/j.ajhg.2007.11.009)
- Murillo-Pineda M, Jansen LET. 2020 Genetics, epigenetics and back again: lessons learned from neocentromeres. *Exp. Cell Res.* **389**, 111909. (doi:10.1016/j.yexcr.2020.111909)
- Hori T, Shang W-H, Takeuchi K, Fukagawa T. 2013 The CCAN recruits CENP-A to the centromere and forms the structural core for kinetochore assembly. *J. Cell Biol.* **200**, 45–60. (doi:10.1083/jcb.201210106)
- Mendiburo MJ, Padeken J, Fülöp S, Schepers A, Heun P. 2011 *Drosophila* CENH3 is sufficient for centromere formation. *Science* **334**, 686–690. (doi:10.1126/science.1206880)
- Bodor DL, Valente LP, Mata JF, Black BE, Jansen LET. 2013 Assembly in G1 phase and long-term stability are unique intrinsic features of CENP-A nucleosomes. *Mol. Biol. Cell* **24**, 923–932. (doi:10.1091/mbc.E13-01-0034)
- Falk SJ *et al.* 2015 Chromosomes. CENP-C reshapes and stabilizes CENP-A nucleosomes at the centromere. *Science* **348**, 699–703. (doi:10.1126/science.1259308)
- Foltz DR, Jansen LET, Black BE, Bailey AO, Yates JR, Cleveland DW. 2006 The human CENP-A centromeric nucleosome-associated complex. *Nat. Cell Biol.* **8**, 458–469. (doi:10.1038/ncb1397)
- Okada M, Cheeseman IM, Hori T, Okawa K, McLeod IX, Yates JR, Desai A, Fukagawa T. 2006 The CENP-H-I complex is required for the efficient incorporation of newly synthesized CENP-A into centromeres. *Nat. Cell Biol.* **8**, 446–457. (doi:10.1038/ncb1396)
- Gascoigne KE, Takeuchi K, Suzuki A, Hori T, Fukagawa T, Cheeseman IM. 2011 Induced ectopic kinetochore assembly bypasses the requirement for CENP-A nucleosomes. *Cell* **145**, 410–422. (doi:10.1016/j.cell.2011.03.031)
- Hori T *et al.* 2008 CCAN makes multiple contacts with centromeric DNA to provide distinct pathways to the outer kinetochore. *Cell* **135**, 1039–1052. (doi:10.1016/j.cell.2008.10.019)
- Silva MCC, Bodor DL, Stellfox ME, Martins NMC, Hochegger H, Foltz DR, Jansen LET. 2012 Cdk activity couples epigenetic centromere inheritance to cell cycle progression. *Dev. Cell* **22**, 52–63. (doi:10.1016/j.devcel.2011.10.014)
- Stankovic A *et al.* 2017 A dual inhibitory mechanism sufficient to maintain cell-cycle-restricted CENP-A assembly. *Mol. Cell* **65**, 231–246. (doi:10.1016/j.molcel.2016.11.021)
- Barnhart MC, Kuich PHJL, Stellfox ME, Ward JA, Bassett EA, Black BE, Foltz DR. 2011 HJURP is a CENP-A chromatin assembly factor sufficient to form a functional de novo kinetochore. *J. Cell Biol.* **194**, 229–243. (doi:10.1083/jcb.201012017)
- Dunleavy EM, Roche D, Tagami H, Lacoste N, Ray-Gallet D, Nakamura Y, Daigo Y, Nakatani Y, Almouzni-Pettinotti G. 2009 HJURP is a cell-cycle-dependent maintenance and deposition factor of

- CENP-A at centromeres. *Cell* **137**, 485–497. (doi:10.1016/j.cell.2009.02.040)
29. Foltz DR, Jansen LET, Bailey AO, Yates JR, Bassett EA, Wood S, Black BE, Cleveland DW. 2009 Centromere-specific assembly of CENP-a nucleosomes is mediated by HJURP. *Cell* **137**, 472–484. (doi:10.1016/j.cell.2009.02.039)
 30. McKinley KL, Cheeseman IM. 2014 Polo-like kinase 1 licenses CENP-A deposition at centromeres. *Cell* **158**, 397–411. (doi:10.1016/j.cell.2014.06.016)
 31. Bodor DL *et al.* 2014 The quantitative architecture of centromeric chromatin. *eLife* **3**, e02137. (doi:10.7554/eLife.02137)
 32. Masumoto H, Masukata H, Muro Y, Nozaki N, Okazaki T. 1989 A human centromere antigen (CENP-B) interacts with a short specific sequence in alphoid DNA, a human centromeric satellite. *J. Cell Biol.* **109**, 1963–1973.
 33. Krenn V, Musacchio A. 2015 The Aurora B kinase in chromosome bi-orientation and spindle checkpoint signaling. *Front. Oncol.* **5**, 225. (doi:10.3389/fonc.2015.00225)
 34. Carmena M, Wheelock M, Funabiki H, Earnshaw WC. 2012 The chromosomal passenger complex (CPC): from easy rider to the godfather of mitosis. *Nat. Rev. Mol. Cell Biol.* **13**, 789–803. (doi:10.1038/nrm3474)
 35. Ambartsumyan G, Gill RK, Perez SD, Conway D, Vincent J, Dalal Y, Clark AT. 2010 Centromere protein A dynamics in human pluripotent stem cell self-renewal, differentiation and DNA damage. *Hum. Mol. Genet.* **19**, 3970–3982. (doi:10.1093/hmg/ddq312)
 36. Jansen LET, Black BE, Foltz DR, Cleveland DW. 2007 Propagation of centromeric chromatin requires exit from mitosis. *J. Cell Biol.* **176**, 795–805. (doi:10.1083/jcb.200701066)
 37. Bodor DL, Rodriguez MG, Moreno N, Jansen LET. 2012 Analysis of protein turnover by quantitative SNAP-based pulse-chase imaging. *Curr. Protocol. Cell Biol.* **55**, 8.8.1–8.8.34. (doi:10.1002/0471143030.cb0808s55)
 38. Pannell D *et al.* 2000 Retrovirus vector silencing is de novo methylase independent and marked by a repressive histone code. *EMBO J.* **19**, 5884–5894. (doi:10.1093/emboj/19.21.5884)
 39. Wood KW, Sakowicz R, Goldstein LS, Cleveland DW. 1997 CENP-E is a plus end-directed kinetochore motor required for metaphase chromosome alignment. *Cell* **91**, 357–366. (doi:10.1016/s0092-8674(00)80419-5)
 40. Cheeseman IM, Chappie JS, Wilson-Kubalek EM, Desai A. 2006 The conserved KMN network constitutes the core microtubule-binding site of the kinetochore. *Cell* **127**, 983–997. (doi:10.1016/j.cell.2006.09.039)
 41. Chan EM *et al.* 2009 Live cell imaging distinguishes bona fide human iPSCs from partially reprogrammed cells. *Nat. Biotechnol.* **27**, 1033–1037. (doi:10.1038/nbt.1580)
 42. Fukagawa T, Earnshaw WC. 2014 The centromere: chromatin foundation for the kinetochore machinery. *Dev. Cell* **30**, 496–508. (doi:10.1016/j.devcel.2014.08.016)
 43. García Del Arco A, Edgar BA, Erhardt S. 2018 *In vivo* analysis of centromeric proteins reveals a stem cell-specific asymmetry and an essential role in differentiated, non-proliferating cells. *Cell Rep.* **22**, 1982–1993. (doi:10.1016/j.celrep.2018.01.079)
 44. Lermontova I, Schubert V, Fuchs J, Klatte S, Macas J, Schubert I. 2006 Loading of *Arabidopsis* centromeric histone CENH3 occurs mainly during G2 and requires the presence of the histone fold domain. *Plant Cell* **18**, 2443–2451. (doi:10.1105/tpc.106.043174)
 45. Ranjan R, Snedeker J, Chen X. 2018 Stem cell mitotic drive ensures asymmetric epigenetic inheritance. *BioRxiv* (doi:10.1101/416446)
 46. Drpic D, Almeida AC, Aguiar P, Renda F, Damas J, Lewin HA, Larkin DM, Khodjakov A, Maiato H. 2018 Chromosome segregation is biased by kinetochore size. *Curr. Biol.* **28**, 1344–1356.e5. (doi:10.1016/j.cub.2018.03.023)
 47. Dunleavy EM, Beier NL, Gorgescu W, Tang J, Costes SV, Karpen GH. 2012 The cell cycle timing of centromeric chromatin assembly in *Drosophila* meiosis is distinct from mitosis yet requires CAL1 and CENP-C. *PLoS Biol.* **10**, e1001460. (doi:10.1371/journal.pbio.1001460)
 48. Fachinetti D, Han JS, McMahon MA, Ly P, Abdullah A, Wong AJ, Cleveland DW. 2015 DNA sequence-specific binding of CENP-B enhances the fidelity of human centromere function. *Dev. Cell* **33**, 314–327. (doi:10.1016/j.devcel.2015.03.020)
 49. Liu L, Michowski W, Kolodziejczyk A, Sicinski P. 2019 The cell cycle in stem cell proliferation, pluripotency and differentiation. *Nat. Cell Biol.* **21**, 1060–1067. (doi:10.1038/s41556-019-0384-4)
 50. Cacchiarelli D *et al.* 2015 Integrative analyses of human reprogramming reveal dynamic nature of induced pluripotency. *Cell* **162**, 412–424. (doi:10.1016/j.cell.2015.06.016)
 51. Koche RP, Smith ZD, Adli M, Gu H, Ku M, Gnirke A, Bernstein BE, Meissner A. 2011 Reprogramming factor expression initiates widespread targeted chromatin remodeling. *Cell Stem Cell* **8**, 96–105. (doi:10.1016/j.stem.2010.12.001)
 52. Ang Y-S *et al.* 2011 Wdr5 mediates self-renewal and reprogramming via the embryonic stem cell core transcriptional network. *Cell* **145**, 183–197. (doi:10.1016/j.cell.2011.03.003)
 53. Bergmann JH, Rodriguez MG, Martins NMC, Kimura H, Kelly DA, Masumoto H, Larionov V, Jansen LET, Earnshaw WC. 2011 Epigenetic engineering shows H3K4me2 is required for HJURP targeting and CENP-A assembly on a synthetic human kinetochore. *EMBO J.* **30**, 328–340. (doi:10.1038/emboj.2010.329)
 54. Miga KH, Newton Y, Jain M, Altemose N, Willard HF, Kent WJ. 2014 Centromere reference models for human chromosomes X and Y satellite arrays. *Genome Res.* **24**, 697–707. (doi:10.1101/gr.159624.113)
 55. Voullaire LE, Slater HR, Petrovic V, Choo KH. 1993 A functional marker centromere with no detectable alpha-satellite, satellite III, or CENP-B protein: activation of a latent centromere? *Am. J. Hum. Genet.* **52**, 1153–1163.